



(12) **EUROPEAN PATENT APPLICATION**

(43) Date of publication:  
**28.08.2024 Bulletin 2024/35**

(51) International Patent Classification (IPC):  
**H01J 49/02<sup>(2006.01)</sup> H01J 49/06<sup>(2006.01)</sup>**

(21) Application number: **23382159.4**

(52) Cooperative Patent Classification (CPC):  
**H01J 49/025; H01J 49/067**

(22) Date of filing: **22.02.2023**

(84) Designated Contracting States:  
**AL AT BE BG CH CY CZ DE DK EE ES FI FR GB GR HR HU IE IS IT LI LT LU LV MC ME MK MT NL NO PL PT RO RS SE SI SK SM TR**  
 Designated Extension States:  
**BA**  
 Designated Validation States:  
**KH MA MD TN**

(72) Inventors:  
 • **BLICK, Robert**  
**20146 HAMBURG (DE)**  
 • **ZIEROLD, Robert**  
**20146 HAMBURG (DE)**  
 • **HAUGG, Stefanie**  
**20146 HAMBURG (DE)**

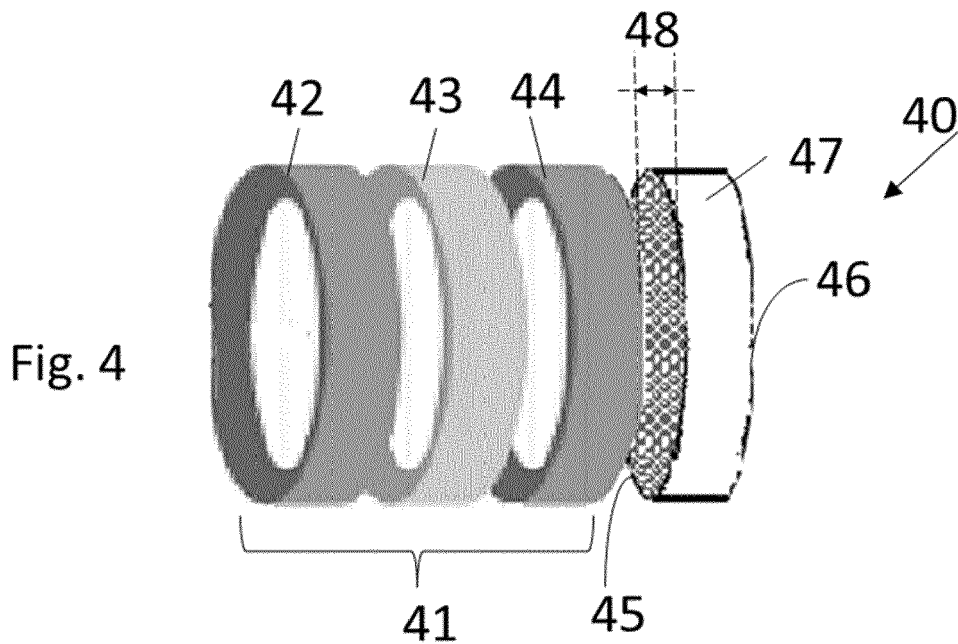
(71) Applicant: **ASOCIACIÓN CENTRO DE INVESTIGACIÓN COOPERATIVA EN NANOCIENCIAS "CIC nanoGUNE"**  
**20018 Donosita-San Sebastián, (ES)**

(74) Representative: **ZBM Patents - Zea, Barlocchi & Markvardsen**  
**Rambla de Catalunya, 123**  
**08008 Barcelona (ES)**

(54) **ACCELERATION UNIT FOR HIGH MASS IONS AND HIGH MASS ION DETECTOR**

(57) There is provided an acceleration unit to accelerate high mass ions, the acceleration unit comprising at least two electrodes separated by an insulation layer for

electrical insulation. There is also provided a high mass ion detector for a mass spectrometer, a mass spectrometer, and a method of detection of high mass ions.



## Description

**[0001]** The present disclosure relates to an acceleration unit to accelerate high mass ions. Besides, a high mass ion detector for a mass spectrometer, a mass spectrometer, and a method of detection of high mass ions are provided.

## BACKGROUND

**[0002]** Top-down proteomics are methods of protein identification which may use an ion trapping mass spectrometer to store an isolated protein ion for mass measurement and tandem mass spectrometry, MS/MS, analysis or may use other protein purification methods such as two-dimensional gel electrophoresis in conjunction with MS/MS. Top-down proteomics deals with the characterization of intact biomolecules, which reduces sample complexity and facilitates the detection of modifications at protein level. The combination of a matrix-assisted laser desorption/ionization, MALDI, technique with time-of-flight, TOF, mass analyzer allows for the generation of gaseous ions in low charge states from high-mass biomolecules, followed by their mass-to-charge ratio ( $m/z$ ) separation, as high-mass ions drift down the flight tube more slowly than lighter ones. Matrix-assisted laser desorption/ionization-time of flight, MALDI-TOF, instruments are widely used for the mass spectrometric analysis of macromolecules. To determine the  $m/z$  values of analytes using MALDI-TOF instruments, the sample is mixed with a matrix that absorbs the energy of a pulsed laser beam and transfers it to the analyte molecules. In this way, ions are usually obtained, which are first accelerated and then pass through a flight tube of known length. Signal amplification is carried out with a secondary electron multiplier, SEM, such as a discrete dynode or a microchannel plate, MCP, from which the analyte ions release electrons upon impact. These electrons are multiplied by means of further dynodes or in individual channels of MCP units. With an anode behind the SEM, an electron shower may be detected.

**[0003]** For example, MCP detectors may be built into MALDI-TOF instruments since MCP detectors are characterized by good time resolution and high sensitivity due to the amplification effect, which may be further improved by using several MCPs in series.

**[0004]** For the separation of individual analyte ions differing in mass and charge in the flight tube of MALDI-TOF devices, all ions may initially receive the same kinetic energy  $E_{kin}$  in an ion source by an acceleration voltage  $U$  applied between MALDI sample plate and the opposing electrode, before entering an electrical field-free TOF mass analyzer. Based on the equation,

$$E_{kin} = q \cdot U = \frac{1}{2} m \cdot v^2 = \frac{1}{2} m \cdot \left(\frac{d}{t}\right)^2$$

high-mass ions have a lower velocity  $v$  than low-mass ions and need more time  $t$  to pass the distance  $d$  of the TOF flight tube, so that the ions can be separated according to their mass  $m$  and charge  $q$ , wherein  $q$  equals an integer number  $z$  of electron charges  $e$ . From the determination of the flight time, the respective  $m/z$  value of the analyte ions can be calculated.

**[0005]** Since the velocity of the ions is inversely proportional to the square root of the ion mass, high-mass molecules exhibit comparatively low velocities. It is known that the probability of secondary electron generation by an ion impact decreases with decreasing ion velocity, leading to a significant reduction of the SEM detection efficiency with increasing ion mass. That means that the conversion of ion-to-electron is reduced, and more secondary ions are generated instead by the impact of the analyte ion on the MCP. For this reason, the signal intensity decreases considerably for higher mass ions, which leads to major limitations in MALDI-TOF applications. This effect is further enhanced in complex samples, since small ions reaching the detector first can also lead to oversaturation of the individual MCP channels.

**[0006]** Some solutions for solving the mentioned inefficiencies of the MCP detectors may comprise cryogenic detectors operated at temperatures  $<100\text{mK}$ . These designs, however, have failed to gain acceptance in routine applications due to the complex and expensive cooling system, and because of their small active detector area. Some approaches to extend the accessible mass range are based on the modification of a conventional MCP detector: either altering the detection mechanism for the electron signal emerging from the backside of the MCP or converting the slow moving, high-mass ions into electrons or into smaller secondary ions before impinging on the MCP frontside. In general, the signal intensity from an MCP detector may be improved by enhancing the velocity of the arriving charged particles, which may be achieved by their acceleration in a large electrical potential. The ions may be accelerated in an ion source of commercial mass spectrometers by voltages of up to 30 kV. A combination of several electrode configurations may be found in order to allow for additional spatial focusing of the ion beam. Higher acceleration voltages in the ion source may risk electrical discharges and may lead to shorter flight times, which in turn require very fast and expensive measurement equipment to achieve sufficient mass resolution.

## SUMMARY

**[0007]** The present disclosure provides examples of devices and methods that at least partially resolve some of the aforementioned disadvantages.

**[0008]** In a first aspect, there is provided an acceleration unit to accelerate high mass ions. The acceleration unit comprises at least two electrodes separated by an insulation layer for electrical insulation. The electrodes

let ions pass through them, for example, through a hole in disk or ring electrodes or in mesh electrodes. In use, ions passing through the electrodes are accelerated due to a voltage potential difference applied to the at least two electrodes. The acceleration unit is configured to operate in a mass spectrometer, which may comprise that the dimensions of the electrodes, for example, an outer dimension of the electrodes is comprised in a range between 10mm and 60mm. For example, an outer diameter of a ring electrode may be comprised in a range between 10mm and 60mm. For example, an outer diameter of a ring insulation layer may be comprised in a range between 10mm and 60mm. In examples, the acceleration unit comprises two electrodes and one insulation layer separating the two electrodes. In examples the acceleration unit comprises 3 electrodes or more. Each pair of electrodes are separated by an insulation layer for electrical insulation, for example if the acceleration unit comprises three electrodes, a first electrode and a second electrode may be separated by a first insulation layer and the second electrode and a third electrode may be separated by a second insulation layer. In use, different voltages may be applied to the 3 or more electrodes such that different combinations of voltage potential differences accelerate ions passing through the electrodes. For example, a first voltage potential difference between a first electrode and a second electrode may accelerate ions by a first acceleration force and a second voltage potential difference between the second electrode and a third electrode may further accelerate the ions by a second acceleration force.

**[0009]** In some examples, the distance defined by the insulation layer between the electrodes may be varied by varying the thickness of the insulation layer. The thickness of the insulation layer may influence the voltage which can be applied to the electrodes to obtain different accelerations for different ions. Ions presenting specific values of  $m/z$  may be accelerated by the acceleration unit of the present disclosure by varying the voltages applied to the electrodes. The insulation layer thickness may govern the breakdown voltage which can be applied to the electrodes in the acceleration unit of the present disclosure. It may be possible, therefore, to design the acceleration unit of the present disclosure such that ions with a mass comprised within a specific range of  $m/z$  values are accelerated as desired. The design may comprise different thicknesses of the insulation layer leading to a unit in which different voltages can be applied to the electrodes to provide specific acceleration forces. The higher  $m/z$  values of the ions to accelerate, the higher voltages are needed and therefore the higher thickness of the insulation layer may be designed.

**[0010]** The acceleration unit of the present disclosure allows, when used with a SEM, taking measurements and detect thereby high mass ions. High mass ions comprise ions with  $m/z$  from  $m/z$  50,000 up to 1,500,000 Daltons, where one Dalton refers to the mass of a single hydrogen atom, but the unit is calibrated to a 1/12 of a

C-12 atom. The  $m/z$  value, in the present disclosure, refers to the mass in Dalton, which is divided by the charging state  $z$  of the ion/protein. In MALDI values for  $z = 1, 2, 3$ , may be found while in ESI  $z$  may be within the order of 50 to 100. The  $z$  may adjust the factor. The acceleration unit may be used by setting zero voltage to the electrodes, which provides an equivalent detection as a detection with a conventional SEM with no acceleration unit. This use corresponds to the acceleration unit being turned off and may be used to compare a detection with and without accelerating unit.

**[0011]** The electrodes may be metallic. The electrodes' geometry may influence acceleration and subsequent detection by a SEM. In examples, the electrodes present a ring shape such that, in operation, a direct line of sight is allowed for the ions to pass through a hole in the ring towards, for example, a SEM. As a skilled person may understand, the ring electrode may present an external and a different internal radius. A mesh electrode may comprise holes which thickness allows ions to pass through.

**[0012]** In a second aspect, there is provided a high mass ion detector for a mass spectrometer, the high mass ion detector comprising: a secondary electron multiplier, SEM, and the acceleration unit of this disclosure. The SEM comprises a front side and a rear side where, in use, the ions enter the front side and may exit the rear side. The SEM may present an outer dimension, for example an outer diameter in the case of ring-shaped SEM, comprised in a range from 20 mm to 60mm, for example outer dimension of 30mm or 40mm or 50mm, or 60mm. In some embodiments, the SEM is an MCP. An MCP comprises a plurality of channels, so that the ions may enter and may exit each channel. The MCP may be used as detector along with a TOF tube in a mass spectrometer. The channels of the MCP may usually be slightly tilted with respect to an axis of the TOF tube, such that a maximum number of ions as possible hit the walls of the MCP and induce electrons into the MCP channels, which may in turn excite further electrons. The ions may remain as debris on the surface of the MCPs. This may lead to finally reducing the responsivity of the MCPs. In some embodiments, the SEM is a dynode, in which case it depends on how the electrodes of the dynodes are arranged, i.e. if they block the TOF line or if they are arranged alongside the line of flight of the TOF. The acceleration unit faces the front side of the SEM and is separated a distance between 100 micrometers and 10mm or from 100 micrometers to 10mm from the front side of the SEM, such that, ions exiting the acceleration unit travel the distance between 100 micrometers and 10mm before impacting the SEM.

**[0013]** The SEM, in use, converts ions into electrons and multiplies the number of electrons inside the SEM.

**[0014]** Conventional detectors usually operate by increasing the acceleration voltage in an ion source. An ion source may comprise a sample of molecules illuminated by a laser. A high mass ion detector according to

this disclosure provides an electrical potential supplied by the electrodes to the ions immediately before, i.e., between 100 micrometers and 10mm before they reach the SEM, electron multiplier or detector, instead of increasing the acceleration voltage in the ion source. A modification on the conventional detector is therefore obtained by the present disclosure.

**[0015]** The high mass ion detector of the present disclosure allows for the amplification of the signal from ionized molecules, or ionized proteins, for example from  $m/z$  50,000 up to 150,000. Ions presenting other values of  $m/z$  also be accelerated by the acceleration unit of the present disclosure by varying the voltages applied to the electrodes. The insulation layer thickness may govern the breakdown voltage which can be applied to the electrodes in the acceleration unit of the present disclosure. The electrodes may be assembled before or in front of a conventional detector SEM. Before or in front of the SEM is to be understood as facing the side of the SEM through which, in use, the ions enter. The electrodes may be set to negative electrical voltages to affect positively charged ions directly before they impinge on the SEM. The electrodes may be set to positive electrical voltages to affect negatively charged ions directly before they impinge on the SEM. The ions are affected by a velocity boost. In some examples, the ions may be further affected by ion optical effects; ion optical effects are to be understood as referring a guidance of charged particles by electrodes in a fashion, similar to conventional optics. The geometry and biasing of the electrode's configuration may be designed to disperse or collimate a beam of ions, for example, charged proteins. Different electrode configurations may be implemented to maximize a detection signal.

**[0016]** The high mass ion detector of the present disclosure may be provided as a plug and play solution to be plugged to a conventional mass spectrometer as will be explained below.

**[0017]** In a third aspect of the disclosure there is provided a mass spectrometer comprising: an ionization region; a time of flight, TOF, tube mass analyzer of a predetermined distance,  $d$ , the TOF tube in communication with the ionization region; and the high mass ion detector of the present disclosure, wherein the high mass ion detector is in communication with the TOF tube, and wherein the acceleration unit of the high mass ion detector is between the TOF tube and the SEM. The mass spectrometer may comprise a laser source configured to illuminate the ionization region, for obtaining ions out of an illuminated sample resting on the ionization region. The laser source may be configured to illuminate a sample for obtaining ions out of the illuminated sample. The laser source may comprise a UV laser, or a nitrogen laser light with a wavelength comprised in a range of nanometers between 340nm and 430nm, for example 337nm or else, i.e., suitable for the applied matrix in MALDI. In use, laser pulses may be fired at matrix crystals mixed with an analyte sample in the form of, for example, dried-droplet spots. The matrix crystals and the analyte mixture may

rest on a plate of the ionization region of the mass spectrometer. The matrix crystals may absorb the laser energy converting the matrix to an ionized state. The charge is transferred to the analyte where a random collision in the gas phase occurs, and the ionized analyte and matrix molecules are desorbed from the plate.

**[0018]** The mass spectrometer further comprises the TOF tube which may comprise an entry zone facing or in communication with the ionization region of the mass spectrometer and an exit zone facing or in communication with the high mass ion detector.

**[0019]** A conventional mass spectrometer may comprise an existing detector. In examples, the high mass ion detector of the present disclosure may be used to replace the existing detector of the conventional mass spectrometer such that, in use, ions formed in the ionization region pass through the TOF tube with an ion flight path and impact the high mass ion detector of the present disclosure. The high mass ion detector of the present disclosure may be placed at the exit zone of the TOF tube to act as a detector of the conventional mass spectrometer. As seen, the high mass ion detector of the present disclosure may be provided as a plug and play solution to be plugged to a conventional mass spectrometer.

**[0020]** When the mass spectrometer according to the disclosure is in use, the ions are affected by the voltages applied to the electrodes before impinging on the SEM, which causes a signal amplification. In use with a mass spectrometer, the high mass ion detector influence analyte ions after they emerge from the TOF tube and shortly before, i.e., between 100 micrometers and 10mm before they hit the SEM surface.

**[0021]** The acceleration unit and the high mass ion detector of the present disclosure may pave the way for increasing the sensitivity of SEM-based detector units for high-mass molecules.

**[0022]** In some examples the SEM is an MCP. In some examples the SEM is a dynode. Advantageously an MCP may be economical to operate and offers rapid response times, narrow pulse widths, high gain, and a sufficiently large active size, which make MCPs good detectors for TOF mass spectrometers.

**[0023]** The present disclosure provides a device and a system to accelerate and thereby to influence analyte ions after they emerge from a TOF tube and shortly before they hit a SEM by adding the acceleration unit -comprising two electrodes separated by an insulating layer- to the detector. In use, a larger signal intensity (25-fold) is generated by a same ion when measured with the high mass ions detector of the present disclosure instead of with the conventional MCP.

**[0024]** In examples, there is provided a method to accelerate ions, comprising: providing an acceleration unit according to the disclosure; applying a voltage potential difference to the at least two electrodes of the acceleration unit; and supplying ions to the acceleration unit; exposing thereby the ions to the voltage potential differ-

ence, which ions are affected by an acceleration force given by the voltage potential difference. The supply of ions may be performed by ionizing a sample analyte.

**[0025]** A fourth aspect of the present disclosure presents a method of detection of high mass ions, the method comprising:

- providing a mass spectrometer, the mass spectrometer comprising an analyte sample;
- ionizing the sample by illuminating the sample with the laser source thereby transferring the sample into a gas phase and releasing charged ions from the sample;
- after all or a part of the charged ions have passed the TOF tube, exposing the charged ions which have passed the TOF tube to voltages applied to the at least two electrodes of the acceleration unit, thereby accelerating the exposed charged ions;
- converting the accelerated charged ions leaving the electrodes into secondary electrons by letting the accelerated charged ions hit the SEM; and
- detecting the presence of high mass ions based on the secondary electrons.

**[0026]** The charged ions may be positively charged ions or negatively charged ions. The positively charged ions may be exposed to a negative potential difference between the voltages applied to the electrodes by passing through the acceleration unit. The negatively charged ions may be exposed to a positive potential difference between the voltages applied to the electrodes by passing through the acceleration unit. Subsequently, ions leaving the acceleration unit, also referred to as booster, are converted to secondary electrons when hitting the SEM surface. Advantageously, a larger signal intensity is generated by a same ion when measured with a detector after the acceleration unit of the present disclosure instead of with an existing conventional detector without the acceleration unit because of a gain in ion velocity in combination with ion optical effects caused by the electrical booster potential provided by the electrodes. An electron shower may accumulate at an anode and a "secondary electron" signal may be measured with an external oscilloscope. In some examples, the SEM is a MCPs in Chevron configuration. In Chevron configuration, the secondary electron signal is amplified by the MCPs in Chevron configuration and the electron shower that accumulates at the anode is measured with the external oscilloscope. In some examples, voltages may be applied independently to the electrodes, which for example may range between zero and -4 kV. Negative voltages advantageously affect the approaching positive ions that emerge from the TOF tube, which improves the signal intensity generated by the SEM.

**[0027]** Advantages derived from these aspects may be similar to those mentioned regarding the first and second aspects.

## BRIEF DESCRIPTION OF THE DRAWINGS

**[0028]** Non-limiting examples of the present disclosure will be described in the following, with reference to the appended drawings, in which:

Figure 1 schematically represents an acceleration unit 10 to accelerate high mass ions.

Figure 2 shows a mesh electrode.

Figure 3 shows a ring electrode.

Figure 4 schematically represents a high mass ion detector 40 according to the present disclosure.

Figure 5 schematically represents a high mass ion detector 40 according to the present disclosure.

Figure 6 represents an example of a conventional mass spectrometer.

Figure 7 represents a mass spectrometer 70 according to the present disclosure.

Figure 8 shows amplification factors, AF, for BSA with three different high mass ion detector examples according to the disclosure.

Figure 9 shows amplification factors, AF, for IgG with three different high mass ion detector examples according to the disclosure.

Figure 10 shows a direct comparison of the mass spectra obtained with the conventional MCPs and with the high mass ion detector of the disclosure.

Figure 11 shows the AF values for higher charge states of BSA ions and of IgG ions.

## DETAILED DESCRIPTION OF EXAMPLES

**[0029]** In these figures the same reference signs have been used to designate matching elements.

**[0030]** Figure 1 shows an acceleration unit 10 to accelerate high mass ions, the acceleration unit comprising at least two electrodes 11, 12 separated by an insulation layer 13 for electrical insulation.

**[0031]** In some examples the insulation layer presents a thickness between 100 micrometers and 6 millimeters, mm, or more particularly, in some examples the insulation layer presents a thickness between 2mm and 6mm or a thickness of 2mm or a thickness of 6mm. The insulation layer may be composed at least in part of an insulating material, for example polytetrafluoroethylene (PTFE), and/or polyetheretherketone (PEEK), and/or Kapton.

**[0032]** In some examples, the high mass detector of the present disclosure may be referred to as booster SEM, referring to the acceleration or "boost" force which, in use, the high mass ion detector impinges on the ions. In some examples the SEM is a Microchannel Plate MCP. In these examples the booster SEM is referred to as a BMCP for "booster MCP". The electrodes' geometry is such that ions are allowed to pass through. For example, figure 1 shows two disk or ring electrodes. The disk electrodes present a hole through which ions pass. The electrodes may present a ring shape or a mesh shape. Figure

2 shows a mesh electrode 20 which, in operation, let the ions pass through the holes in the mesh. Other configurations are covered by the present disclosure as long as ions can pass through the electrodes, in use. A circular shape, for example disk or ring shape allows that, in use and when applying a voltage potential difference to ions passing through the holes of the electrodes, the ions form an oblate or prolate cloud of ions (depending on the ionization, acceleration, and dispersion during propagation), which is guided and/or altered by the electrical field. In the case of disk or ring shaped electrodes as shown in figure 3, an electrode may comprise an external diameter 31 of for example between 50 mm and 60mm or between 2 inches to 3 inches, and an internal diameter of for example between 20 mm and 30 mm or from 1 inch to 1,5 inches.

**[0033]** In use, a disk or ring shape electrode provides a direct line of sight to the detector, which in examples may be a SEM, or an MCP. This advantage may become clear in the following examples according to this disclosure. The electrodes in the acceleration unit may present different shapes: for example, a first electrode may be a mesh electrode and a second electrode may be a ring electrode. A third electrode may be a square electrode presenting a hole letting ions pass through. The holes letting ions pass through the electrodes may be aligned from an electrode to the rest of electrodes. The holes letting ions pass through the electrodes may not be aligned from an electrode to the rest of electrodes, in which case ions may divert the path travelled from one electrode to the following one.

**[0034]** Figure 4 schematically represents a high mass ion detector 40 according to the present disclosure. The high mass ion detector comprises, as shown in figure 4, a secondary electron multiplier, SEM 47, for converting ions into electrons and for multiplying the number of electrons inside the SEM, where the SEM comprises a front side 45 and a rear side 46 where, in use, the ions enter the front side; and the acceleration unit 41 separated a distance 48, between 100 micrometers and 10mm from the front side of the SEM. The acceleration unit 41 of figure 4 comprises a first electrode 42, an insulation layer 43 and a second electrode 44. In operation, as seen in figure 5, the ions travelling in the direction of the arrow, enter the high mass ion detector 40 through the first electrode 42 and may exit through the rear side. Ions exiting the acceleration unit travel the distance between 100 micrometers and 10mm before impacting the SEM 47. As shown in figure 5, electrons 53 exiting the SEM may accumulate in an anode 52 and the electron shower may be detected.

**[0035]** The example shown in figures 4 and 5 show two circular electrodes or booster electrodes. The electrodes may be separated by polytetrafluoroethylene (PTFE) plates for electrical insulation. The SEM shown in figures 4 and 5 is a microchannel plates MCP. In examples, two MCP assembled in Chevron configuration are used. The figure 5 shows a metal anode 52. The elements may be

fixed together by polyetheretherketone (PEEK) screws and nuts, and may sit on an electrical insulated base, for example, a PTFE pedestal for electrical insulation from a vacuum flange underneath.

5 **[0036]** Figure 6 shows an example of a conventional mass spectrometer showing a laser source 61, a matrix with analyte 62, a ionization region 63, a TOF tube 64 in which ions travel in the direction of the arrow and are separated according to their mass or  $m/z$  values, and an  
10 MCP detector 65.

**[0037]** Figure 7 shows a mass spectrometer 70 according to the present disclosure, comprising an ionization region 73; a laser source 71 configured to illuminate the ionization region, for obtaining ions 75 out of an illuminated sample 72 resting on the ionization region; a time of flight, TOF, tube mass analyzer 74, the TOF tube in communication with the ionization region 73 such that ions are allowed to pass from the ionization region to the TOF tube; and the high mass ion detector 40 according to this disclosure, wherein the high mass ion detector is in communication with the TOF tube, and wherein the acceleration unit 41 of the high mass ion detector is between the TOF tube 74 and the SEM 47. As it may become apparent, the MCP detector 65 of figure 6 may be replaced by the high mass ion detector 40 according to the present disclosure to obtain a mass spectrometer 70 according to the present disclosure. As seen, despite the acceleration unit extension, the ions still have direct access to the SEM's surface.

20 **[0038]** In operation, a power supply or two or more power supplies may be used. Two first separate power supplies may be used to apply negative voltages to each of the electrodes, for example up to -4 kV. A third power supply may be coupled to a voltage divider circuit to set an input of the SEM to ground. In examples where the SEM comprises two microchannel plates MCP assembled in Chevron configuration, the third power supply may be coupled to a voltage divider circuit to set an input of the first MCP to ground and the second MCP to about  
25 +1.8 kV and the anode to +2 kV for positive ion detection. Strong potentials may be obtained by combining more than 2 electrodes. The configuration may be flexible depending on the application needs.

30 **[0039]** Compared to the conventional SEM detector, the signal intensity provided by the high mass ion detector of the present disclosure is amplified by a factor of 24.3 for a charged bovine serum albumin, BSA (BSA,  $\geq 98\%$ , molecular weight 66 400 u) BSA ion ( $m/z$  66 400) and of 10.7 for a charged immunoglobulin G, IgG, from human serum (IgG,  $\geq 95\%$ , molecular weight 150 000 u) IgG ion ( $m/z$  150 000) and above to the MDa-range.

35 **[0040]** In examples, different voltages may be applied independently to the electrodes, for example between zero and -4 kV in 1 kV steps, and different distances defined by the insulation layer, for example a PTFE spacer, between the electrodes are constructed. The different combinations of configurations may provide different results. For example, this allows testing a configuration that

yields the largest signal intensification for a particular application and with a particular sample analyte. In an example, a 6 mm thick insulation layer was used, called "large distance configuration" example. In a second example, called "medium distance configuration" example, a 2mm thick insulation layer was used. In a third example, called "short distance configuration" example, a 10 microns-insulator layer was used, which may perform as a "zero spacing" acceleration unit -or short distance configuration, which combined with setting zero voltage to the electrodes, corresponds to the acceleration unit being turned off.

**[0041] SAMPLE PREPARATION** Experiments performed comprised the use of the standard proteins bovine serum albumin (BSA, ≥98%, molecular weight 66 400 u) and immunoglobulin G from human serum (IgG, ≥95%, molecular weight 150 000 u), acetone, acetonitrile, acetonitrile with 0.1% trifluoroacetic acid (TFA) and water with 0.1% TFA (all LC-MS grade), both MALDI matrices α-cyano-4-hydroxycinnamic acid (α-CHCA) and 2,5-dihydroxybenzoic acid (DHB), formic acid (≥99%, LC-MS grade), water purified using an on-site purification system). Initially, various protocols were evaluated for MALDI sample preparation, all of which use manual pipetting for the matrix deposition on the target plate. First, the two proteins BSA and IgG were dissolved in 0.1% TFA in water and adjusted to a concentration of 3.0 μmol L<sup>-1</sup> and of 1.3 μmol L<sup>-1</sup>, respectively. For the MALDI matrix, 7.0 mg of α-CHCA were added to 100 μL of acetone to prepare a saturated solution. Using a 10 μL pipette tip, which was briefly wetted with this solution, a thin layer was applied to the MALDI target (ground steel) and allowed to dry. Furthermore, 20 mg α-CHCA were dissolved in 1 mL of a mixture of acetonitrile and 5% formic acid in water (70:30, v/v). Also, 20 mg DHB was taken up in 1 mL of a mixture of acetonitrile and 0.1% TFA in water (70:30, v/v). These two solutions were mixed in a ratio of 1:1 (v/v). Subsequently, either 2 μL of the BSA or 2 μL of the IgG protein solution were briefly mixed with 2 μL of the solution of α-CHCA and DHB. From this obtained new solution, 0.5 μL was added to the thin layer of α-CHCA. The spots were left to dry in ambient conditions and were then measured directly.

**[0042] MEASUREMENTS.** The measurements were carried out on a modified ultrafleXtreme MALDI TOF/TOF system in linear positive ion mode. The instrument is equipped with a smartbeam 2 laser. The control of the MALDI source took place via the software flexControl (Bruker Daltonics). The used method was optimized for the measurement of m/z values in the range of 30 000 to 210 000 with the discrete dynode detector of the mass spectrometer and was provided by the manufacturer of the instrument (U =25 kV acceleration voltage, 460 ns pulsed ion extraction). The measurements were performed in the positive polarity mode and 100 laser shots at a frequency of 20 Hz were averaged to obtain one mass spectrum. The detector side of the mass spectrometer was modified by removing the discrete dynode de-

tector and replacing it by the high mass ion detector 40 according to the present disclosure. A load lock chamber was installed for convenient exchange of the detectors. Calibration measurements with the conventional MCP detector revealed an adjusted flight path length of about d = 2.21 m. The high mass ion detector 40 according to the present disclosure comprised: Two circular booster electrodes, referred to as BEs, separated by polytetrafluoroethylene (PTFE) plates for electrical insulation, two microchannel plates MCPs assembled in Chevron configuration (F1552-01, Hamamatsu Photonics, Hamamatsu City, Japan) and a metal anode. The assembly was fixed by polyetheretherketone (PEEK) screws and nuts, and was sitting on a PTFE pedestal for electrical insulation from the vacuum flange underneath. Each initial measurement was performed at least 24 h after mounting the high mass ion detector 40 according to the present disclosure in high vacuum (below 2·10<sup>-5</sup> Pa) to allow for proper degassing and thus, to lower the risk for electrical discharge in the MCPs. To supply the electrical voltages to the individual components of the high mass ion detector according to the disclosure, three external high voltage power supplies were used. Separate power supplies were used to apply negative voltages to each of the two booster electrodes BEs (up to -4 kV). The third device was coupled to a voltage divider circuit to set the input of the first MCP to ground, the second MCP to about +1.8 kV and the anode to +2 kV A capacitor was assembled between the anode and an external oscilloscope (DSO9254A, Keysight Technologies, Santa Rosa, CA, USA) to suppress any DC current noise and to acquire only the AC signal produced by impinging ions. The oscilloscope input was set to 1 MΩ for impedance matching between the oscilloscope and the rest of the circuit to provide a better signal response. An external oscilloscope was used to record the signal amplitude in volts as a function of the flight time and the trigger signal from the mass spectrometer was sent to one channel of the oscilloscope to mark the zero-flight time. Then, the signal was acquired for 500 μs (500 MSa s<sup>-1</sup> sample rate, 250 kSa sample size). To obtain a single mass spectrum, the signal generated by 100 laser shots was averaged using the averaging function of the oscilloscope. The voltages applied to the MCP-anode assembly were held constant, but the voltages provided to the two electrodes were varied independently between zero and -4 kV to maximize the signal intensity generated by arriving ions.

**[0043] DATA PROCESSING** Before further evaluation of the measured data, the flight time may be converted to the m/z value using the following equation:

$$\frac{m}{z} = \frac{2 e U}{u} \cdot (t/d)^2$$

with acceleration voltage U, for example U = 25 kV; the determined flight path length of d, for example d = 2.21

m; the electron charge  $e = 1.602 \cdot 10^{-19}$  C; and the atomic mass unit  $u$ , for example  $u = 1.661 \cdot 10^{-27}$  kg.

**[0044]** Subsequently, the baseline of the mass spectrum was corrected using the function "msbackadj" from MATLAB (MathWorks, Natick, MA, USA). Then, the intensities of the peaks in the mass spectrum were extracted using the function "mspeaks" for determination of the signal enhancement caused by the different voltage- and distance-configurations tested for the High mass ion detector according to the disclosure in comparison to the conventional MCP assembly. The intensity variations of the signal generated by a singly bovine serum albumin (BSA+1, at about  $m/z$  66 400) and by doubly (BSA+2, at about  $m/z$  33 200) charged BSA ions were investigated in dependence on the change of the booster electrode, BE, voltages for the three high mass ion detector distance configurations -large distance configuration, medium distance configuration and zero spacing or short distance configuration. Note that the present disclosure may refer the "zero spacing distance" or "short distance configuration" when using a 10 microns-insulator layer, which may perform as a "zero spacing" acceleration unit -or short distance configuration, which combined with setting zero voltage to the electrodes, corresponds to the acceleration unit being turned off. Five mass spectra were obtained for each voltage combination. Mean intensity values and the standard deviations were derived from the five mass spectra per voltage combination for the singly and doubly charged BSA ions in order to account for the changes in signal intensity that are typically related to local deviations of the MALDI sample quality ("sweet spots"). To allow for the direct comparison of the acquired mass spectra, amplification factors (AFs) were determined by normalizing the peak intensities measured with the high mass ion detector of the disclosure, also referred to as BMCP for "booster MCP", to the value that was obtained with the BEs turned off, namely with the conventional MCP detector. The errors of the AFs were derived by Gaussian error propagation using the standard deviations of the peak intensities for calculation.

**[0045]** Figure 8 shows amplification factors, AF, for BSA with three different high mass ion detector examples according to the disclosure. The AFs found for the large electrode separation are shown in Fig. 8(a), for the medium one in Fig. 8(b) and for the measurements with zero electrode spacing in Fig. 8(c). The AFs for the doubly charged and singly charged BSA ions are presented in the top and bottom row of the image, respectively. For the large and the medium electrode separation, all combinations of electrode voltages between zero and -4 kV were tested in 1 kV steps. Note, for the booster configuration with zero electrode separation-resulting in a single electrode-only one high voltage power supply was used to apply the voltages between zero and -4 kV in 1 kV steps. In the following, the results for the doubly charged BSA ion will first be compared for the different electrode distances. Subsequently, the AFs derived for the singly charged BSA ion will be contemplated. For the large BE

distance shown in Figure 8(a), a maximum amplification factor, AF, of  $3.4 \pm 1.0$  was found for -3 kV at the bottom and -4 kV at the top BE, and also for the reverse voltage combination. A reduced AF of  $2.0 \pm 0.7$  was obtained for -4 kV at both electrodes. The largest AF of  $13.4 \pm 7.4$  for BSA+2 was found for the medium electrode distance with -3 kV at the bottom and -4 kV at the top BE, as shown in Figure 8(b). Similar to the results for the large electrode separation, a comparable AF was derived for the reverse voltage combination and a slightly lower AF was found when the same voltage of -4 kV was applied to both BEs. Furthermore, a local maximum of  $9.1 \pm 5.3$  was noticed for -2kV at the bottom and -1 kV at the top BE. For zero electrode distance, the AF varied between  $3.9 \pm 2.1$  and  $4.4 \pm 3.7$  with changing the electrodes voltage. Note, the signal intensity for -4 kV was not sufficient to derive a value for the AF. Similar observations as for the doubly charged BSA ion were made for the singly charged BSA ion as shown in the bottom row of Fig 8. Again, the largest AF of  $24.3 \pm 8.9$  was obtained for the medium electrode spacing (Fig. 8(b)) for a combination of -3 kV at the bottom and -4 kV at the top BEs. Slightly lower AFs were found for the reverse voltage combination and for -4 kV applied to both BEs. Additionally, a local maximum was also discovered at the voltage combination of -2 kV and -1 kV at the bottom and the top electrode, respectively, yielding an AF of  $15.0 \pm 8.6$ . Significantly lower AF values were observed for the large electrode separation (Fig. 8(a)) as well as for zero electrode separation (Fig. 8(c)). The largest AF of  $13.4 \pm 14.7$  obtained for the large electrode spacing with -3 kV at the bottom electrode and the top electrode turned off, may possibly be treated as an outlier. In general, a larger signal amplification was achieved with a higher negative voltage applied to the BEs, independently of the used detector configuration. It is assumed that the observed behavior was generated by an increased acceleration of the positively charged ions with rising negative booster voltage, by ion optical effects, or by a combination of both effects.

**[0046]** On the one hand, a higher negative voltage will likely cause a stronger acceleration of the positively charged ions before they hit the MCP surface. Thus, the AF enhancement may be related to the well-known increase of the MCP detection efficiency with rising ion velocity. The strongest signal intensification for singly and doubly charged BSA ions was observed for the medium electrode separation (Fig. 8(b)). On the other hand, one could identify two well-known-but opposite-ion optical mechanisms that could have led to the observed signal amplification: First, the used electrode configuration may cause-aside from the intended ion acceleration-a certain spatial focusing of the ion beam, as it was noticed for other electrode configurations beforehand. Second, the negative electrode booster potential may lead to an ion beam divergency. Thus, the positively charged ion cloud would cover a larger area of the active MCP surface, which may be favorable with regard to the relatively long dead time (millisecond range) of the single channels.

Note, only one of these two opposing ion optical effects may have contributed to the observed increase in signal intensity.

**[0047]** Compared to the findings for the medium spacing, the AFs were reduced for the large electrode separation. In this configuration, the BEs may be too far apart from each other to efficiently accelerate and focus the ions. Possibly, the positively charged ions are attracted by and consequently hit the negative BEs instead of reaching the MCPs because of the extended flight path through the booster. Thus, less ions would have reached the MCP surface for the large electrode distance, which may have led to the observed reduction in signal intensity compared to the medium electrode separation.

**[0048]** The AFs found for zero electrode separation are in general larger than the values observed for the large electrode spacing. However, the signal amplification is significantly smaller than for the medium electrode configuration. Thus, it is expected that the single BE (zero electrode spacing) causes a velocity enhancement for the ions, but may not have a distinct influence on the spatial distribution of the ion beam. Typically, assemblies that are designed for ion beam focusing consist of several electrostatic lenses, like the three-element einzel lens, which is a combination of tubular acceleration lenses with opposite polarity.

**[0049]** The strongest signal amplification was not observed for the highest voltage (-4 kV) applied to both booster electrodes simultaneously, but at a booster voltage combination of -3 kV/4 kV (bottom/top BE). It is possible that this voltage combination creates an electric field gradient that has an effect on the spatial extent of the ion beam and appears to lead to enhanced detection efficiency at the MCPs. Additionally, local maxima were detected at voltages below -4 kV for the large as well as for the medium electrode separation. Accordingly, the maximum voltages at the BEs are not necessary to achieve a significant signal amplification by the High mass ion detector according to the disclosure. Moreover, a shift of the local maximum was observed for the AF measured for singly and for doubly charged BSA ions when the detector configuration was changed from medium to large electrode separation. This observation may indicate an effect of the length of the insulating layer between the two BEs on the ion beam focusing properties of the booster.

**[0050]** In conclusion, figure 8 shows signal amplification of singly and doubly charged BSA ions for three booster electrode configurations. The separation between the top and the bottom electrode, provided by an insulation layer, was changed from (a) a large distance, to (b) a medium distance, and finally, (c) to zero distance between the two electrodes. The strongest amplification was noticed for the medium electrode spacing. The peak intensities found for BSA+2 and BSA+1 were normalized to the measurements with the electrode voltages turned off to extract the signal amplification. The dark gray spaces indicate the absence of a detectable signal. Further,

please note the different amplitudes in the color-coded 3D plots.

**[0051]** Figure 9 shows amplification factors, AF, for IgG with three different high mass ion detector examples according to the disclosure. The AFs for IgG were derived from the measurements with the BMCP in the three different configurations as previously explained for BSA. The results for the doubly (IgG +2, at about m/z 75 000) and for the singly (IgG+1, at about m/z 150 000) charged IgG ions are summarized in the top and in the bottom row of Fig. 9, respectively. The AFs are given in Fig. 9(a) for the large electrode distance, in Fig. 9(b) for the medium one, and in Fig. 9(c) for zero electrode separation.

**[0052]** First, the results for the doubly charged IgG ion and second, the observations for the singly charged IgG ion are discussed in the following. For the large electrode separation (Fig. 9(a)), the largest AF of  $2.4 \pm 2.0$  for IgG+2 was found for a bottom/top electrode voltage combination of -2 kV/-4 kV. However, the AFs found for -4 kV at both electrodes as well as for both variants of -3 kV/-4 kV, vary within this standard deviation of the AF for -2 kV/-4 kV. For the medium electrode separation (Fig. 9(b)), a much larger AF of  $23.6 \pm 14.6$  was found for -3 kV/-4 kV at the bottom/top BEs. Slightly lower AF values were obtained for the reverse voltage combination, and for -4 kV applied to both BEs. Additionally, a local maximum of  $11.1 \pm 6.6$  was measured for 2 kV/-1 kV at bottom/top BEs. For zero electrode separation (Fig. 9(c)), large variations of the AF between  $1.7 \pm 1.3$  and  $6.8 \pm 6.0$  were noticed for IgG+2.

**[0053]** For the singly charged IgG ion, a maximum AF of  $7.2 \pm 0.2$  was observed at -4 kV at the bottom and -3 kV at the top BE using the large electrode separation, shown in the bottom row of Fig. 9(a). The AF was found to be smaller for the reverse voltage combination and for -4 kV at both BEs. A local maximum of 5.8 was found for -2 kV/-1 kV at the bottom/top BEs. Since the intensity of the signal measured with the booster turned off was not sufficient to be detected and thus to calculate an AF, the peak intensities were normalized to the value found for -1 kV at the bottom electrode and zero volts at the top electrode. For the medium electrode configuration in Fig. 9(b), a maximum AF of  $10.7 \pm 5.2$  was found for -4 kV/-3kV at the bottom/top BEs. For the other BE voltage combinations, comparable trends were observed as for the previously described results of IgG +2 measured with medium electrode distance. For zero electrode separation (Fig. 9(c)), no reliable signal amplification was observed as the AFs vary between  $0.2 \pm 0.2$  and  $1.2 \pm 2.1$ .

**[0054]** Similar to the observations for BSA in Fig. 8, the AFs generally increase with rising applied voltage at the BEs, which could be related to the enhancement in MCP detection efficiency with rising ion velocity and ion focusing effects. Additionally, the medium electrode separation yielded also for IgG the strongest signal intensification compared to the two other BE configurations. The AF decreased only slightly from BSA+1 at about m/z 66 400 to IgG+2 at about m/z 75 000, namely from 24.3 to

23.7.

**[0055]** However, a significantly lower AF of 10.7 was found for IgG +1 that appears at a much larger m/z of about 150000. This decrease in AF with increasing m/z value is an expected behavior, since the acceleration voltages at the BEs are the same for all approaching ions. Thus, the higher mass ions are still slower than the lighter ones when impinging on the MCP surface, which causes the mass-dependent detection efficiency of the MCPs. Note that the largest AF of the doubly charged IgG on (at about m/z 75 000) was found for a combination of -3 kV at the bottom and -4 kV at the top BE, which is similar to the observations made for the doubly charged BSA ion (at about m/z 33 200) and for the singly charged BSA ion (at about m/z 66 400). However, the strongest amplification for the singly charged IgG ion (at about m/z 150 000) was obtained for the reverse BE voltage combination of -4 kV/-3 kV (bottom/top BE). It is known that the expansion of the ion cloud in vacuum is assumed to increase with ion mass in the TOF mass analyzer, leading to a loss of control over the ions' spatial distribution for higher mass ions. Hence, the effect of the electrical booster potential on the spatial extension of the ions is probably mass dependent, as ion clouds with different masses may approach the booster with different degrees of lateral expansion.

**[0056]** Furthermore, the local maxima for the medium electrode separation were observed with -2 kV at the bottom and -1 kV at the top BE for BSA+2, BSA+1, as well as for IgG+2. Only for the singly charged IgG ion another local maximum was observed at a voltage combination of -3 kV/-1 kV at the bottom/top BEs, which may be related to a mass-dependent ion beam expansion.

**[0057]** In conclusion, figure 9 shows signal amplification of singly and doubly charged IgG ions for three booster electrode configurations. The separation between the top and the bottom electrode, provided by an insulation layer, was changed from (a) a large distance, to (b) a medium distance, and finally, (c) to zero distance between the two electrodes. The strongest amplification was again noticed for the medium electrode spacing. The peak intensities found for IgG +2 and IgG +1 were normalized to the measurements with the booster voltages turned off to extract the signal amplification, and the gray spaces indicate the absence of a detectable signal. However, the peak intensities measured with the large electrode distance for IgG +1 were normalized to the signal for -1kV at the bottom and zero voltage at the top electrode, since no sufficient peak intensity was detected for both electrode voltages turned off.

**[0058]** From the three tested electrode configurations, the medium BE spacing yielded the largest amplification for the signal generated by the boosted ions upon impact on the MCP surface. This configuration seems to cause an efficient ion acceleration, and possibly also a convenient focusing of the ion beam, which results in an enhanced signal intensity compared to the conventional MCP detector. Since the detection mechanism relies on

the conversion of analyte ions into secondary electrons using MCPs, the velocity of the ions is still determining the detection efficiency. Thus, it is expected that the AF reduces with increasing ion mass, since the higher mass ions will still be slower than the lighter ones, as all ions experience the same electrical potential when traversing through the BEs. Figure 10 shows a direct comparison of the mass spectra obtained with the conventional MCPs, plotted in a solid line at the bottom of the graphics, and with the BMCP having a medium electrode spacing plotted in a line over the previous line, showing the strong signal enhancement achieved. The detected signal was enhanced the most for -3 kV at the bottom and -4 kV at the top BE for BSA Fig. 10(a), plotted in the top line, and for the reverse voltage combination for IgG Fig. 10(b), plotted in the top line. Furthermore, a local maximum of the AF was observed for both proteins with the combination of -2 kV at the bottom and -1 kV at the top BE.

**[0059]** However, using the same voltage at both BEs did not cause the strongest signal enhancement, for -3 kV and for -4 kV. In the following, the discussion will focus on the mass spectra obtained for the booster settings that yielded the largest signal amplification for BSA and IgG in comparison to the results for the booster part turned off. The signal for the doubly and singly charged BSA ion, see Fig. 10(a), was amplified by a factor of 15.5 and of 27.0, respectively, when detected with the BMCP, plotted in the top line instead of with the conventional MCP, plotted in the lower line. The voltage combination of -3 kV at the bottom and -4 kV at the top BE yielded the largest AFs for BSA. Additionally, the mean peak intensity and the corresponding standard deviation are shown for BSA +2 and for BSA +1 indicate the variation among the five mass spectra obtained for this voltage combination. For the doubly charged BSA ion, the mean intensity rose from  $0.0016 \pm 0.0007$  to  $0.0218 \pm 0.0072$ , and for the singly charged BSA ion, the intensity increased from  $0.0009 \pm 0.0002$  to  $0.0210 \pm 0.0057$  when using the BMCP. Thus, the absolute change in signal intensity for successively measured mass spectra was found to increase with the AF values and therefore, with the BE voltages. Moreover, the full width at half maximum (FWHM) was derived for the peaks attributed to the singly and to the doubly charged BSA ions in Fig. 10(a) as a measure for the change of mass resolving power when using the BMCP instead of the MCP detector. The FWHM increased from 1 300 u to 1 900 u for the signal at m/z 33 200 (BSA 2+) and decreased from 4 300 u to 2 900 u for the signal at m/z 66 400 (BSA 1+) when the BMCP instead of the conventional MCP detector was used. A frequency of 20 Hz for firing the laser may be used to average the signal produced by 100 single laser shots. Possibly, modifications of the BMCP detector measurement, such as the upgrade of the data acquisition system, may allow for a direct comparison of the conventional system and the MCP/BMCP detector according to the disclosure.

**[0060]** Fig. 10(b) compares a single mass spectrum of

IgG measured with the conventional MCP (lower line) to one that was acquired with the high mass ion detector according to the disclosure (top line). For the shown mass spectra, AF values of 14.3 for IgG +2 and of 9.2 for +1 IgG were found with -4 kV at the bottom and -3 kV at the top BEs. The mean signal intensity of the five mass spectra at this voltage combination rose for the doubly charged IgG ion from  $0.0009 \pm 0.0003$  to  $0.0141 \pm 0.0049$ , and for singly charged IgG ion from  $0.0009$  to  $0.0099 \pm 0.0048$ . Again, an increase of the signal intensity variation is noticed with rising AF value and thus, with growing BE voltages. The FWHM increased from 3 700 u to 4 200 u for the signal at  $m/z$  75 000 (IgG 2+), and it was reduced from 10 800 u to 3 500 u for the signal at  $m/z$  150 000 (IgG1+) when using the high mass ion detector according to the disclosure. The change of the FWHM with BE setting is shown for both proteins. No significant variations of the  $m/z$  values were observed for the different ions with changing BE voltage combinations.

**[0061]** Increasing of the acceleration voltage in the ion source may be the obvious way to further improve the MCP detection efficiency. However, the applied voltage is in practice limited by the increase of the in-source ion decay with increasing acceleration voltage. Hence, the increase of the intensity variations with rising BE voltage may be related to an enhanced probability for fragmentation of the ions when passing through the booster electrodes for acceleration. Furthermore, the variation in peak width with changing BE voltage may be related to the spatial distribution of the ion beam. For instance, a reduction in ion mass resolution was reported elsewhere for the combined use of a conversion dynode and a post-acceleration stage compared to the conventional MCP detector. The observed reduction in resolution was attributed to the influence of the post-acceleration stage on the ion beam. The overall reproducibility of the measurements with the high mass ion detector according to the disclosure may be improved by applying other matrix deposition methods than the herein used manual pipetting. Other matrix deposition techniques, such as sublimation and nebulization, are known to generate MALDI samples with enhanced homogeneity and with increased purity of the deposited matrix, which could reduce the observed signal intensity variation. Comparison of peak intensities for BSA and IgG revealed a mass dependent decrease in signal intensity. The mean AF derived for the singly charged BSA ion (24.3) decreased by about 56% for the singly charged IgG ion (10.7). Thus, the higher mass IgG ion will still arrive at the MCP surface with a slower velocity than the lower mass BSA ion, causing the mass-dependent MCP detection efficiency. In addition, it cannot be ruled out that the decrease in signal intensity for IgG is also related to the spatial expansion of the ion cloud when approaching the booster extension at the MCP detector. Since the ion cloud expansion in vacuum is supposed to increase with ion mass, the decrease in signal intensity could also be related to the loss of higher mass ions when colliding with the BEs instead

of reaching the MCP. Additionally, several peaks below the  $m/z$  values of the doubly charged BSA ion ( $<m/z$  33 200) and of the doubly charged IgG ion ( $<m/z$  75 000) were noticed in the two mass spectra in Fig. 10, which are assumed to correspond to higher charge states of BSA and IgG. A similar observation has already been made by Choi et al., whereby a strong correlation with the used MALDI matrix was observed. Since the multiply charged ions were observed for the MCP as well as for the BMCP measurements, their occurrence is likely related to other influences, such as the properties of the used matrix type. When comparing the AF found for the doubly charged BSA ion ( $m/z$  33 200) with the value found for the doubly charged IgG ion ( $m/z$  75 000), an increase from 13.4 to 23.7 is observed, which indicates a dependence of the AF on the  $m/z$  value.

**[0062]** Figure 11 shows the AF values for higher charge states of BSA ions and of IgG ions. The figure can be separated into the following three  $m/z$  regions: First, the signal amplification generated by the booster seems to work most efficient for ions within the  $m/z$  range of about 50 000 - 75 000 and second, the AF decreases for ions having a  $m/z$  value above about 75 000 because of the mass-dependent MCP detection efficiency. Third, for  $m/z$  values below about 50 000, the AF reduces with decreasing  $m/z$  value. The ions with lower  $m/z$  values have a larger velocity than ions with higher  $m/z$  values, since the ion's velocity is inversely proportional to the square root of their  $m/z$  value. Hence, the accelerating effect of the booster on the ions with lower  $m/z$  values may be smaller, because they travel through the booster part faster. Possibly, the reduction of the relative AF with increasing ion velocity (smaller  $m/z$  values) is caused by a less effective acceleration generated by the booster than for slower moving ions that have larger  $m/z$  values. Note, investigation of other ionized molecules in the future could reveal further details on the observed dependence of the relative signal amplification on the  $m/z$  value.

**[0063]** Conclusions: an extension of the conventional MCP detector was used for signal amplification of standard protein ions up to at least  $m/z$  150 000. Three configurations of the high mass ion detector according to the disclosure were tested to maximize the amplification factor. The medium electrode separation provided the largest signal enhancement by generating a convenient combination of acceleration of the positively charged ions by the negative booster electrodes with ion optical effects. It is likely that the spatial ion beam distribution is affected by the electrical booster potential causing the enhanced signal intensity observed for this BMCP configuration in contrast to the two other designs. In general, the signal amplification got stronger for larger applied booster voltages. However, the largest amplification factors were found for combinations of -3 kV and -4 kV at the booster electrodes. Additionally, a local amplification factor maximum was detected for the voltage combination of -2 kV at the bottom and -1 kV at the top booster electrode, which offers the possibility to operate the high mass ion

detector according to the disclosure with enhanced sensitivity already at electrical potentials of maximum 2 kV. The absolute signal intensity was found to decrease with increasing mass. This behavior is to be expected since the same booster voltage was used for all masses and thus, the higher mass ions will remain slower than the lighter ones after passing the booster stage. Nevertheless, the influence of the booster part proved to be sufficient to allow reliable detection of m/z values of up to 150000. The accessibly m/z range of the BMCP may be extended by application of larger electrical voltages to the booster electrodes. Note, the herein presented concept is not limited to proteins but could be applied to the analysis of high-mass substances, e.g., polymers and dendrimers, too.

**[0064]** Additionally, a mass gate may be used in combination with the high mass ion detector according to the disclosure to avoid saturation of the MCP channels by the pulsed deflection of the first arriving low-mass ions, which could lead to further enhancement of the signal generated by high mass ions. Such an experiment may require a fast switch (in the order of a few microseconds) between zero (or low) applied voltages to high voltages.

**[0065]** For reasons of completeness, various aspects of the present disclosure are set out in the following numbered clauses:

Clause 1. A high mass ion detector for a mass spectrometer, the high mass ion detector comprising:

- a secondary electron multiplier, SEM, for converting ions into electrons and for multiplying a number of electrons inside the SEM, where the SEM comprises a front side and a rear side where, in use, the ions enter the front side; and
- an acceleration unit separated a distance between 100 micrometers and 10 millimeters from the front side of the SEM; wherein the acceleration unit comprises at least two electrodes, wherein each pair of electrodes are separated by an insulation layer for electrical insulation; and
- wherein the acceleration unit is separated a distance between 100 micrometers and 10 millimeters from the front side of the SEM.

Clause 2. The high mass ion detector of clause 1 wherein the insulation layer presents a thickness between 100 micrometers and 10 millimeters.

Clause 3. The high mass ion detector of any one of clauses 1 or 2 wherein the insulation layer presents a thickness of 2mm or a thickness of 6mm.

Clause 4. The high mass ion detector of any one of clauses 1 to 3 wherein at least one of the electrodes and/or one of the insulation layers present a circular shape or a ring shape.

Clause 5. The high mass ion detector of any one of clauses 1 to 4 wherein a first electrode and a second electrode are separated by a first insulation layer and the second electrode and a third electrode are separated by a second insulation layer.

Clause 6. A mass spectrometer comprising:

- an ionization region;
- a laser source configured to illuminate the ionization region, for obtaining ions out of an illuminated sample resting on the ionization region;
- a time of flight tube, TOF tube, mass analyzer, the TOF tube in communication with the ionization region; and
- the high mass ion detector of any one of clauses 1 to 5, wherein the high mass ion detector is in communication with the TOF tube, and wherein the acceleration unit of the high mass ion detector is between the TOF tube and the SEM of the high mass ion detector.

Clause 7. A method to accelerate ions, comprising:

- providing an acceleration unit which comprises at least two electrodes, wherein the acceleration unit is configured to operate in a mass spectrometer, the acceleration unit comprising at least two electrodes, and wherein each pair of electrodes are separated by an insulation layer for electrical insulation;
- applying a voltage potential difference to the at least two electrodes of the acceleration unit; and
- supplying ions to the acceleration unit; exposing thereby the ions to the voltage potential difference, which ions are affected by an acceleration force given by the voltage potential difference.

Clause 8. The method to accelerate ions of clause 7 wherein the supplying of ions is performed by ionizing a sample analyte.

Clause 9. A method of detection of high mass ions, the method comprising:

- providing a mass spectrometer according to clause 6, the mass spectrometer comprising an analyte sample;
- ionizing the analyte sample and releasing charged ions from the analyte sample;
- after all or a part of the charged ions have passed the TOF tube, exposing the charged ions which have passed the TOF tube to voltages applied to the at least two electrodes of the acceleration unit, thereby accelerating the exposed charged ions;
- converting the accelerated charged ions leaving the electrodes into secondary electrons by let-

ting the accelerated charged ions hit the SEM;  
and

- detecting a presence of high mass ions based on the secondary electrons.

Clause 10. The method of clause 9 wherein ionizing the analyte sample is performed by illuminating the sample with a laser source thereby transferring the sample into a gas phase.

**[0066]** Although only a number of examples have been disclosed herein, other alternatives, modifications, uses and/or equivalents thereof are possible. Furthermore, all possible combinations of the described examples are also covered. Thus, the scope of the present disclosure should not be limited by particular examples but should be determined only by a fair reading of the claims that follow.

### Claims

1. An acceleration unit to accelerate high mass ions, the acceleration unit configured to operate in a mass spectrometer, the acceleration unit comprising at least two electrodes, and wherein each pair of electrodes are separated by an insulation layer for electrical insulation.
2. The acceleration unit of claim 1 wherein the insulation layer presents a thickness between 100 micrometers and 10 millimeters.
3. The acceleration unit of claim 2 wherein the insulation layer presents a thickness of 2mm or a thickness of 6mm.
4. The acceleration unit of any one of claims 1 to 3 wherein the insulation layer is composed at least in part of polytetrafluoroethylene (PTFE).
5. The acceleration unit of any one of claims 1 to 4 comprising two electrodes, wherein a first electrode and a second electrode are separated by a first insulation layer.
6. The acceleration unit of any one of claims 1 to 4 comprising three electrodes, wherein a first electrode and a second electrode are separated by a first insulation layer and the second electrode and a third electrode are separated by a second insulation layer.
7. The acceleration unit of any one of claims 1 to 6 wherein at least one of the electrodes and/or each of the insulation layers present a circular shape or a ring shape.
8. A high mass ion detector for a mass spectrometer,

the high mass ion detector comprising:

- a secondary electron multiplier, SEM, for converting ions into electrons and for multiplying a number of electrons inside the SEM, where the SEM comprises a front side and a rear side where, in use, the ions enter the front side; and
- the acceleration unit of any of claims 1 to 7 separated a distance between 100 micrometers and 10 millimeters from the front side of the SEM.

9. A mass spectrometer comprising:

- an ionization region;
- a time of flight tube, TOF tube, mass analyzer, the TOF tube in communication with the ionization region; and
- the high mass ion detector of claim 8, wherein the high mass ion detector is in communication with the TOF tube, and wherein the acceleration unit of the high mass ion detector is between the TOF tube and the SEM of the high mass ion detector.

10. A method of detection of high mass ions, the method comprising:

- providing a mass spectrometer according to claim 9, the mass spectrometer comprising an analyte sample;
- ionizing the analyte sample, releasing charged ions from the analyte sample;
- after all or a part of the charged ions have passed the TOF tube, exposing the charged ions which have passed the TOF tube to voltages applied to the at least two electrodes of the acceleration unit, thereby accelerating the exposed charged ions;
- converting the accelerated charged ions leaving the electrodes into secondary electrons by letting the accelerated charged ions hit the SEM; and
- detecting a presence of high mass ions based on the secondary electrons.

11. The method of claim 10 wherein exposing the charged ions to voltages applied to the at least two electrodes comprises applying a voltage to at least one of the electrodes.

12. The method of claim 11 wherein the voltage applied to the at least one of the electrodes ranges from 0KV to -4 KV.

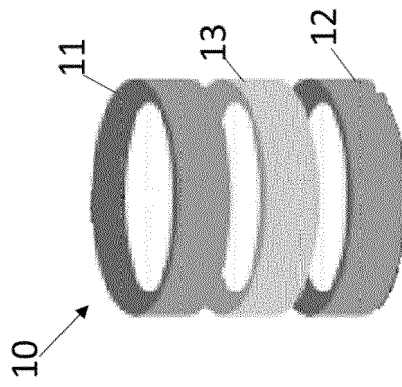


Fig. 1

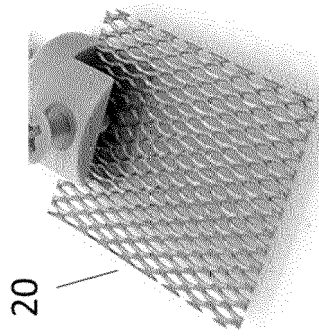


Fig. 2

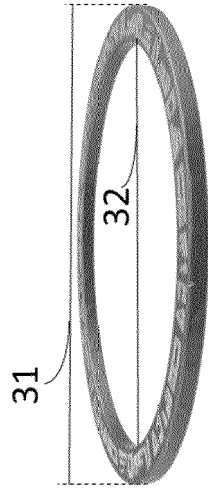
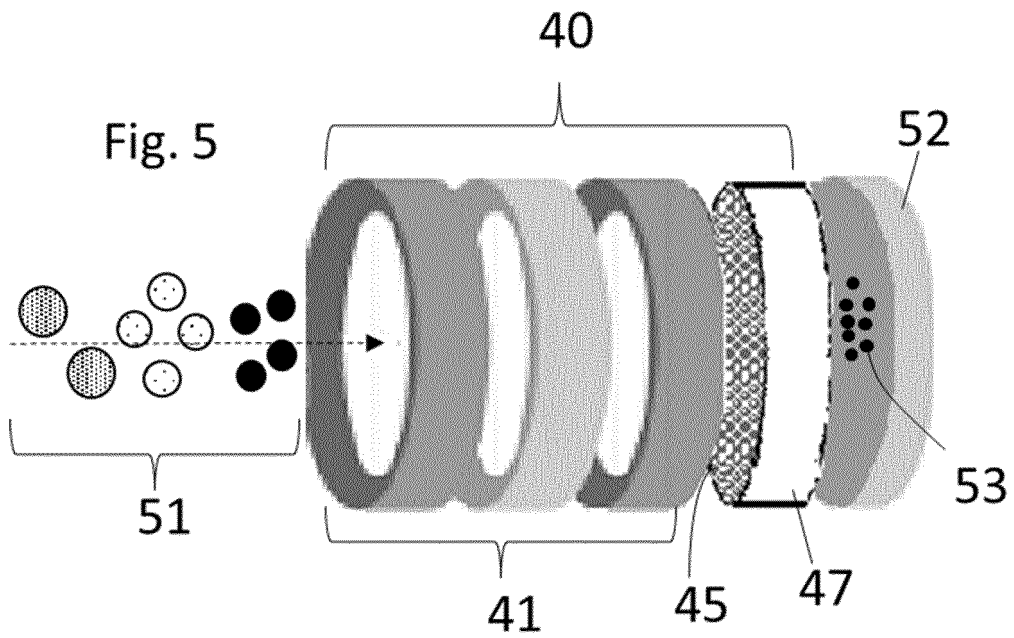
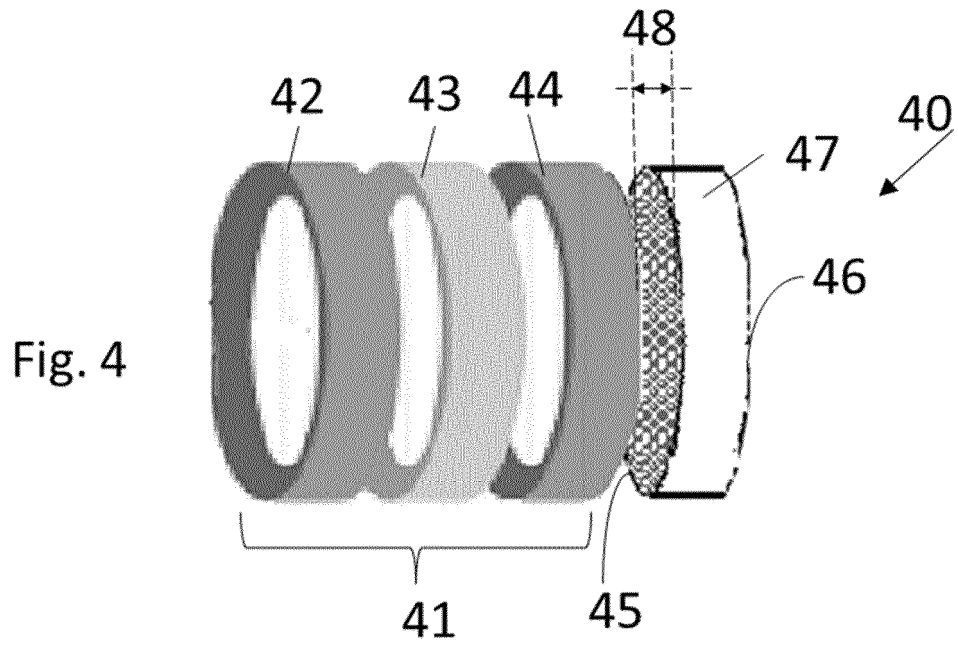
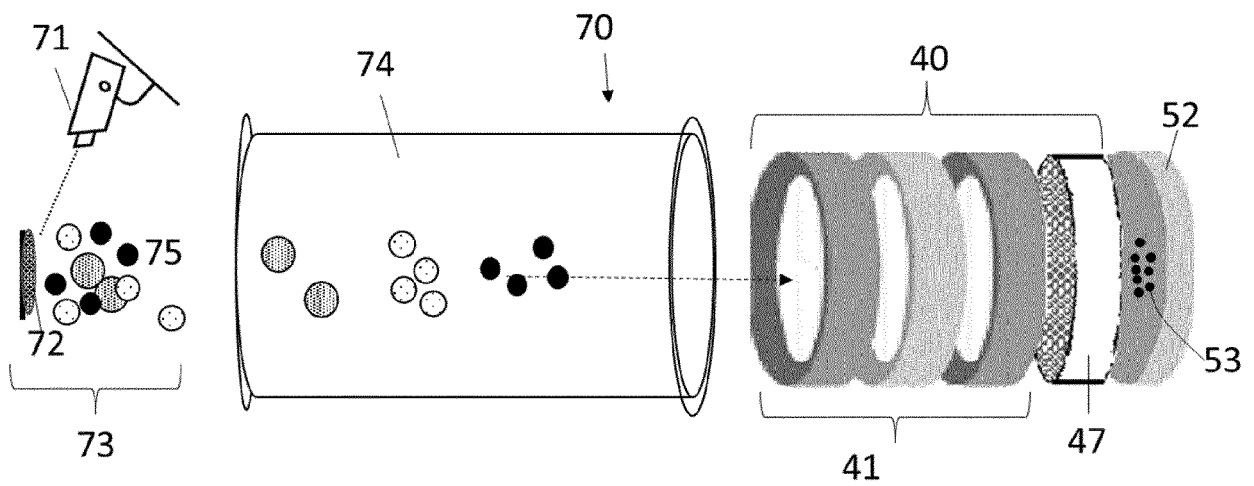
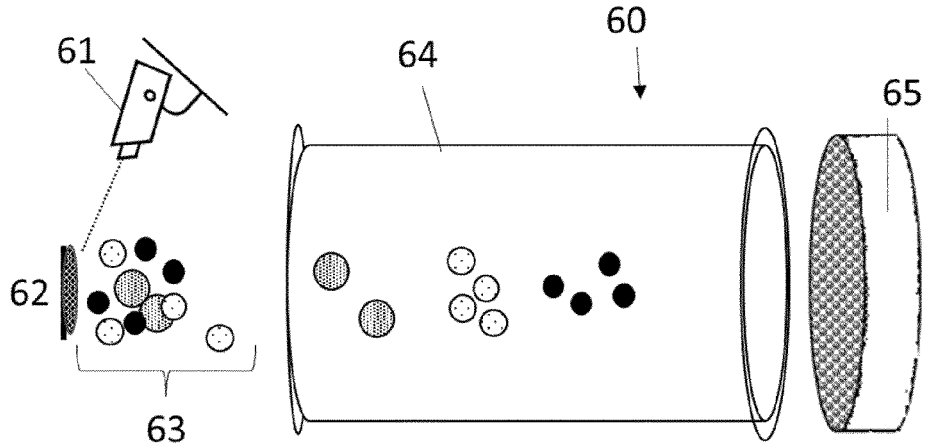


Fig. 3





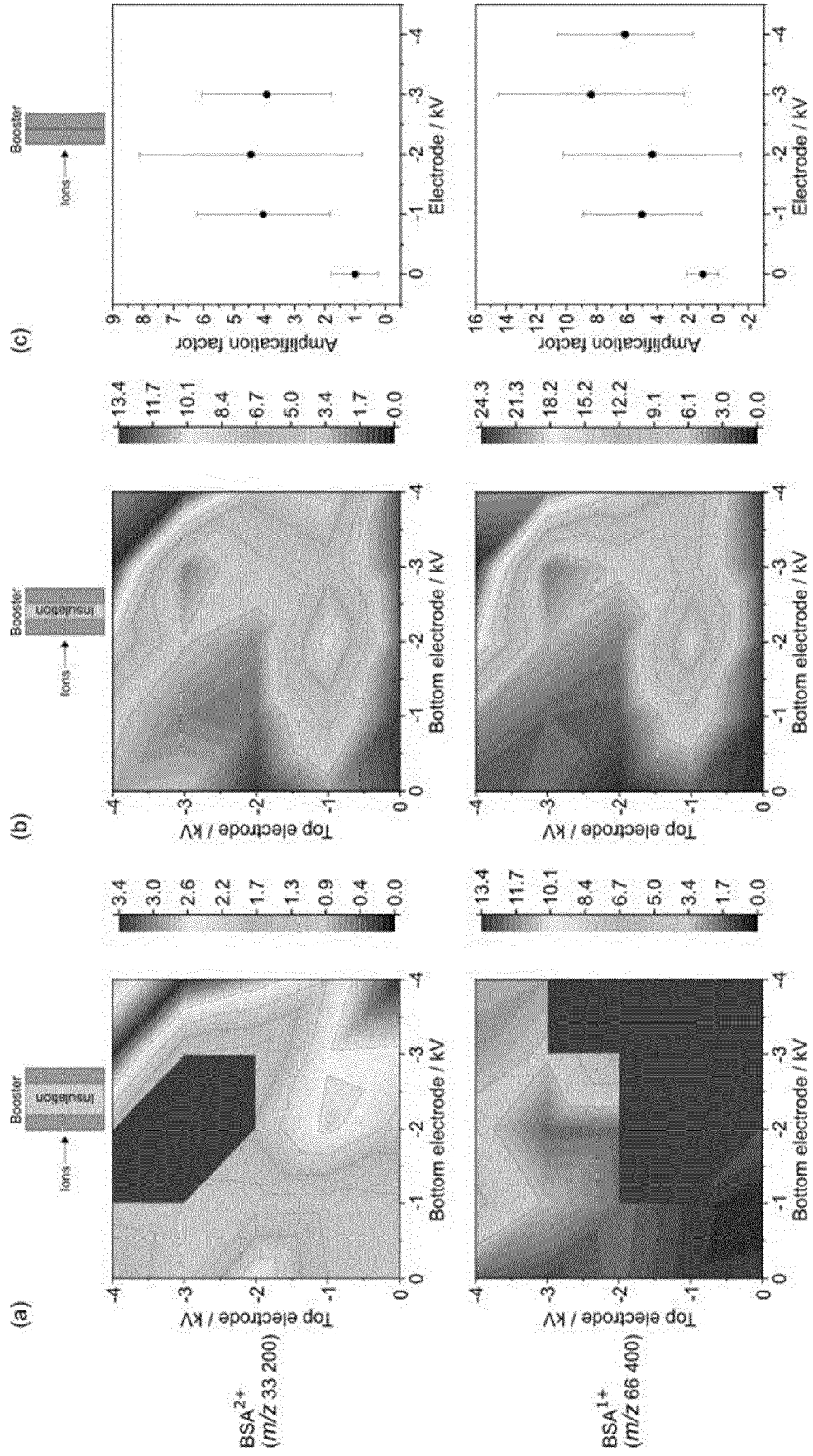


Fig. 8

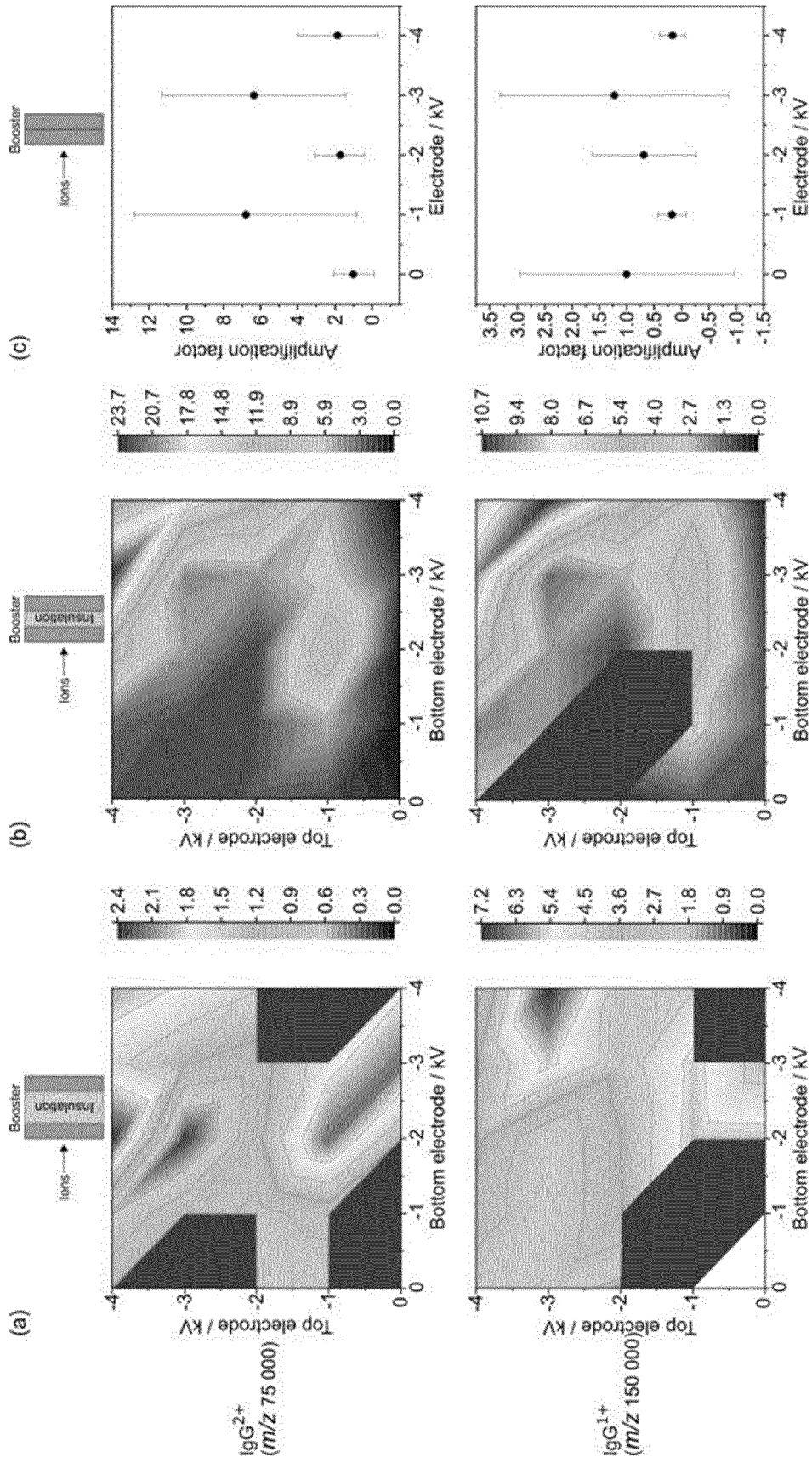


Fig. 9

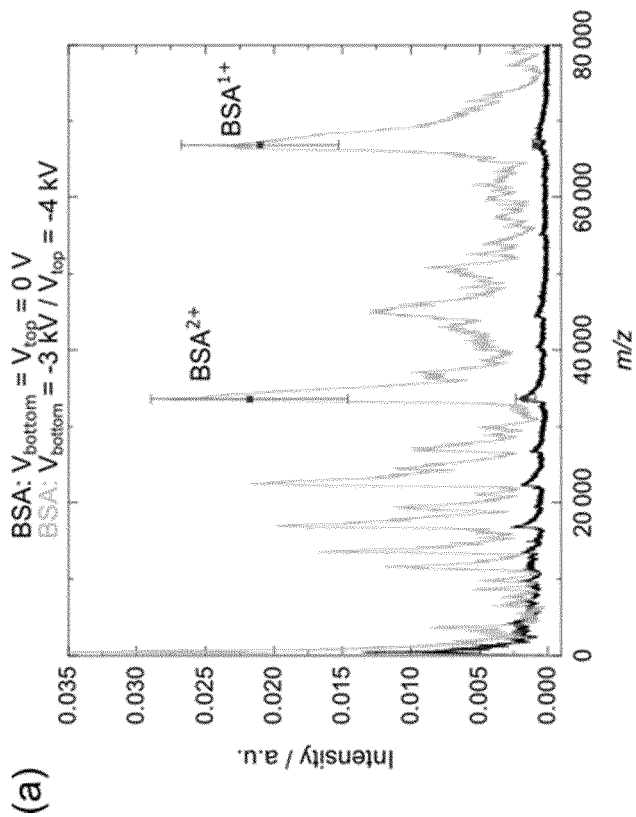
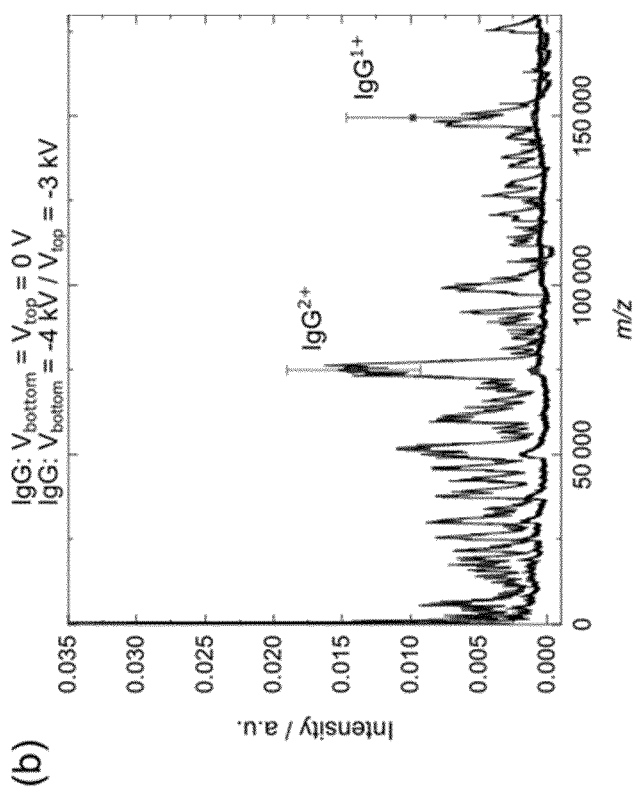


Fig. 10

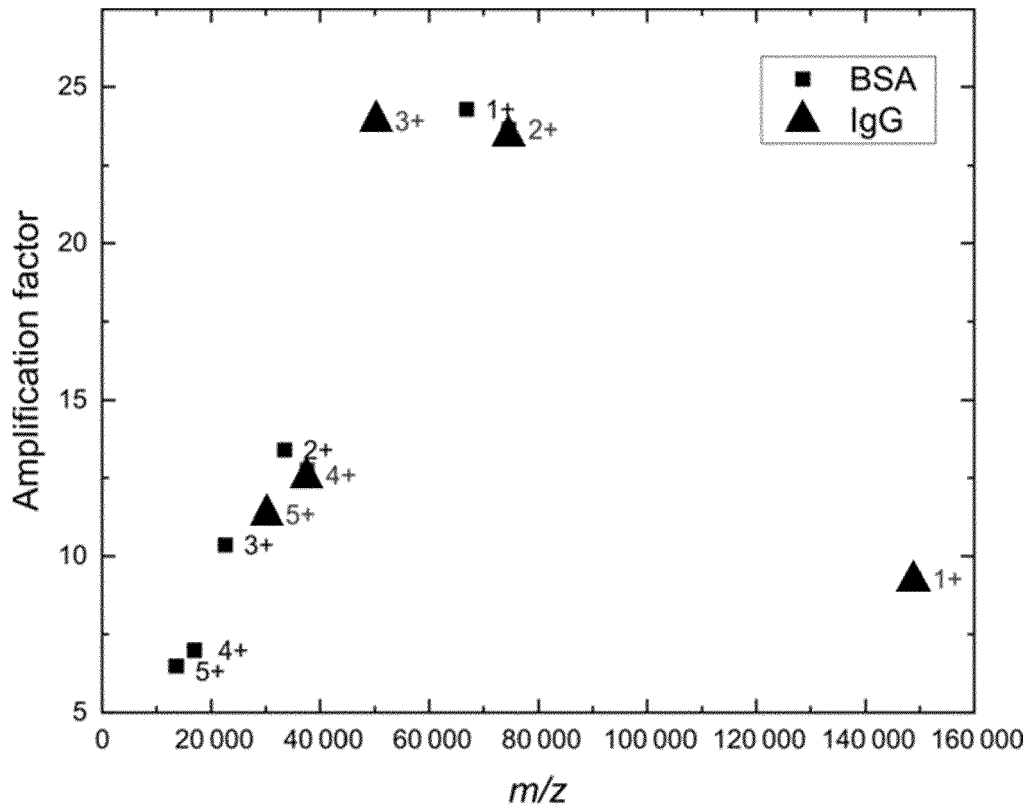


Fig. 11



EUROPEAN SEARCH REPORT

Application Number

EP 23 38 2159

5

10

15

20

25

30

35

40

45

50

55

DOCUMENTS CONSIDERED TO BE RELEVANT			
Category	Citation of document with indication, where appropriate, of relevant passages	Relevant to claim	CLASSIFICATION OF THE APPLICATION (IPC)
X	WO 2011/048061 A2 (THERMO FISHER SCIENT BREMEN [DE]; MAKAROV ALEXANDER [DE] ET AL.) 28 April 2011 (2011-04-28) * claims 1, 18; figures 3, 6 * * page 41, line 26 - page 42, line 4 * -----	1-12	INV. H01J49/02 H01J49/06
X	WO 2021/003888 A1 (GUANGZHOU HEXIN INSTR CO LTD [CN] ET AL.) 14 January 2021 (2021-01-14) * paragraph [0033] - paragraph [0036]; figure 2 * * paragraph [0002] * -----	1-12	
X	EP 3 629 365 A1 (IONICON ANALYTIK GES M B H [AT]) 1 April 2020 (2020-04-01) * paragraphs [0070], [0072]; figure 2 * -----	1-7	
X	US 2021/242007 A1 (VERENCHIKOV ANATOLY [ME]) 5 August 2021 (2021-08-05) * claims 33,36,37 * -----	1-7	
X	EP 2 131 386 A1 (SHIMADZU CORP [JP]) 9 December 2009 (2009-12-09) * paragraphs [0024], [0030], [0039]; figure 3 * -----	1-7	TECHNICAL FIELDS SEARCHED (IPC) H01J
The present search report has been drawn up for all claims			
Place of search <b>The Hague</b>		Date of completion of the search <b>10 July 2023</b>	Examiner <b>Peters, Volker</b>
CATEGORY OF CITED DOCUMENTS X : particularly relevant if taken alone Y : particularly relevant if combined with another document of the same category A : technological background O : non-written disclosure P : intermediate document		T : theory or principle underlying the invention E : earlier patent document, but published on, or after the filing date D : document cited in the application L : document cited for other reasons ..... & : member of the same patent family, corresponding document	

1  
EPO FORM 1503 03.82 (P04C01)

ANNEX TO THE EUROPEAN SEARCH REPORT  
ON EUROPEAN PATENT APPLICATION NO.

EP 23 38 2159

5 This annex lists the patent family members relating to the patent documents cited in the above-mentioned European search report.  
The members are as contained in the European Patent Office EDP file on  
The European Patent Office is in no way liable for these particulars which are merely given for the purpose of information.

10-07-2023

Patent document cited in search report	Publication date	Patent family member(s)	Publication date
WO 2011048061 A2	28-04-2011	CA 2777810 A1	28-04-2011
		CN 102782800 A	14-11-2012
		EP 2491573 A2	29-08-2012
		JP 5684274 B2	11-03-2015
		JP 2013508905 A	07-03-2013
		US 2011095178 A1	28-04-2011
		WO 2011048061 A2	28-04-2011
WO 2021003888 A1	14-01-2021	CN 112216592 A	12-01-2021
		WO 2021003888 A1	14-01-2021
EP 3629365 A1	01-04-2020	CN 111971779 A	20-11-2020
		EP 3629365 A1	01-04-2020
		EP 3776629 A1	17-02-2021
		US 2021057203 A1	25-02-2021
		WO 2020065012 A1	02-04-2020
US 2021242007 A1	05-08-2021	CN 111902908 A	06-11-2020
		EP 3782186 A1	24-02-2021
		JP 7299238 B2	27-06-2023
		JP 2021518045 A	29-07-2021
		US 2021242007 A1	05-08-2021
		WO 2019202338 A1	24-10-2019
EP 2131386 A1	09-12-2009	EP 2131386 A1	09-12-2009
		JP 4883174 B2	22-02-2012
		JP WO2008117333 A1	08-07-2010
		US 2010096541 A1	22-04-2010
		WO 2008117333 A1	02-10-2008